Analytical Methods

Accepted Manuscript

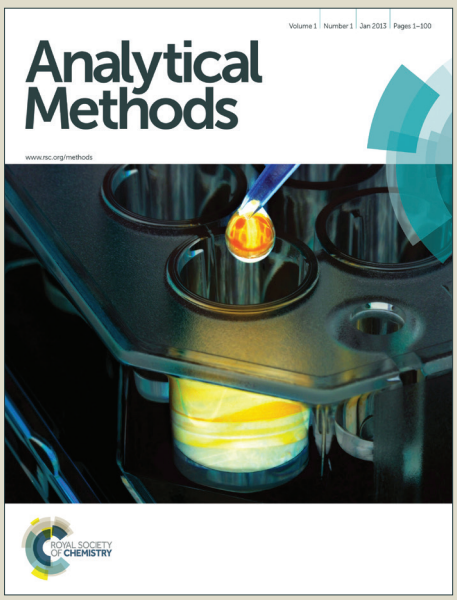

ROYAL SOCIETY OF CHEMISTRY

www.rsc.org/methods

$NiFe_2O_4$ nanoparticles decorated with MWCNTs as a selective and sensitive electrochemical sensor for the determination of epinephrine using differential pulse voltammetry

Ali A. Ensafi*[1], F. Saeid[1], B. Rezaei[1], Ali R. Allafchian[2]

1. *Department of Chemistry, Isfahan University of Technology, Isfahan 84156–83111, Iran*
2. *Nanotechnology and Advanced Materials Institute, Isfahan University of Technology, Isfahan 84156–83111, Iran*

Abstract

A glassy carbon electrode was modified with nickel-ferrite magnetic nanoparticles and decorated with multiwall carbon nanotubes ($NiFe_2O_4$–MWCNTs). Differential pulse voltammetry was then used to investigate the electrochemical behavior of epinephrine at the surface of the modified electrode. The properties of the nanocomposite were also characterized using different techniques. The electrode showed an excellent synergic effect on epinephrine oxidation. At the optimum pH level, the electrode's response in 0.1 mol L^{-1} phosphate solution was proportional to the concentration of epinephrine in the range of 0.9 – 800.0 μmol L^{-1} with a detection limit of 0.09 μmol L^{-1}. The effects of different potentially interfering substances on the epinephrine signal were also studied. Finally, the sensor was evaluated with respect to its reproducibility and stability. It was found that the modified electrode has a good sensitivity, selectivity, and reproducibility for the determination of epinephrine in real samples.

* Corresponding author: Tel.: +98–311–3913269; Fax: +98–311–3912350; E–mail: Ensafi@cc.iut.ac.ir

Keywords: $NiFe_2O_4$–MWCNTs; Synergic effect; Epinephrine determination; Differential pulse voltammetry.

1. Introduction

Nanoparticles coming in different sizes, shapes, and compositions are nowadays revolutionizing the field of bioanalytical measurement. Nickel ferrite ($NiFe_2O_4$) with an inverse spinel structure shows ferrimagnetism that originates from the magnetic moment of anti-parallel spins between Fe(III) ions at tetrahedral sites and Ni(II) ions at octahedral sites.[1] Y.L. Liu et al.[2] reported a hydrogen sulfide sensor based on $NiFe_2O_4$ nanopowder doped with noble metals. L. Yang et al.[3] prepared $NiFe_2O_4$ by inverse titrating chemical co-precipitation and studied the electrical and gas-sensing characteristics of the material using several gases such as hydrogen. L. Luo et al.[4] reported on a glucose biosensor based on $NiFe_2O_4$ nanoparticles and chitosan.

Carbon nanotubes (CNTs) have received increasing attention due to their unique mechanical, chemical, and electrical properties such as high electrical conductivity and high surface area to mass ratio.[5–9] Numerous applications of CNTs–modified sensors have been used in electrochemical sensors.[10–17] Decoration of CNTs films with spinel ferrite nanoparticles with the chemical formula MFe_2O_4 (M = Mn, Co, Ni, Mg, or Zn)[18–20] improves the electrochemical properties of the nanocomposite to create high performance electrochemical sensors.[2-5]

Epinephrine (known as adrenaline) is one of the most important catecholamine neurotransmitters for the message transfer in the mammalian central nervous system, which is released by the adrenal gland under conditions of low blood sugar levels or in reaction to

psychological stresses.[21–23] It has important functions in the regulation of physiological processes in living systems, treatment of myocardial infarction, bronchial asthma, hypertension, and cardiac surgery.[24] The quantitative determination of epinephrine is, therefore, important not only in nerve physiologic functions but also as a diagnostic and control clinical medicine.[24]

Several methods have been reported for the determination of epinephrine including high performance liquid chromatography (HPLC),[25,26] HPLC-mass spectrometry,[27] fluorimetry,[28] HPLC-optical fiber biosensor,[29] capillary electrophoresis,[30,31] flow injection,[32,33] HPLC with fluorimetric detection,[34] chemiluminescence,[35,36] spectrophotometry[37,38] and electrochemical methods.[39-46]. Electrochemical techniques are suitable for the detection of epinephrine due to their sensitivity, rapidity, accuracy, and low cost. For these reasons, different modified electrodes have been introduced for the detection of epinephrine that include gold electrode,[42] ionic liquid modified carbon nanotubes paste electrode,[43] MnO_2–Nafion modified glassy carbon electrode,[44] glassy carbon electrode modified with carbon fiber ultra microelectrode[45], and graphene/gold nanocomposite modified-glassy carbon electrode.[46]

Nanoparticles based transition metals oxide[44] and/or spinel ferrite nanoparticles with a chemical formula of MFe_2O_4 are good candidates[20] to develop electrochemical sensors for detecting of important biological compounds. These electrochemical sensors are good selectivity, tunable electron transport properties with fast analytical response. In the present work, a new electrochemical sensor is introduced for the electrochemical detection of epinephrine. The sensor is based on multiwall carbon nanotubes decorated with $NiFe_2O_4$ nanoparticles ($NiFe_2O_4$–MWCNTs) at a surface of glassy carbon electrode (GCE).[47,48]

Differential pulse voltammetry (DPV) is used as a suitable technique for the determination of epinephrine. The results show that the nanocomposite has a synergic effect on the oxidation of epinephrine. The sensor exhibits a good sensitivity, low detection limit, good stability and free from interference of ascorbic acid and uric acid *vs.* the reported electrochemical methods for epinephrine detection (Table 1). It has been successfully used for the determination of epinephrine in pharmaceutical and urine samples with satisfactory results. **"Here Table 1"**

2. Experimental

2.1. Reagents

All chemicals used were of analytical grade and used as received without further purification. All chemicals were purchased from Sigma (St. Louis, USA) otherwise stated. Doubly distillate water was used for preparation of all the solutions.

Written informed consent was obtained from all participants prior to the collection of samples.

Epinephrine was purchased from Aldrich (Milwaukee, USA) and was used without further purification. MWCNTs was purchase from Aldrich Chemicals (Milwaukee, USA) with diameter of 70 – 110 nm and length of 5 – 9 μm. $NiFe_2O_4$ nanoparticles (particle size, 20–40 nm) were synthesized in our laboratory. A colloidal suspension of $NiFe_2O_4$ nanoparticles was prepared by dispersing of $NiFe_2O_4$ nanoparticles in methanol in an ultrasonic water bath for 20 min before use.

0.010 mol L^{-1} epinephrine solution was prepared daily by dissolving 0.0183 g of epinephrine in water containing 500 μL HCl (37% w/w) and the resulting solution was diluted with water, then it kept in a refrigerator at 4 ^{o}C before use.

Phosphate solutions (sodium hydrogen phosphate and disodium monohydrogen phosphate plus sodium hydroxide, 0.1 mol L^{-1}) with different pH values were used. All solutions were prepared in double distillated water.

2.2. Apparatus

All electrochemical experiments were performed with a Metrohm instrument (Herisau, Switzerland), Model 799 VA processor. A conventional three-electrode electrochemical system was used, which consisted of a working electrode ($NiFe_2O_4$–MWCNTs-modified glassy carbon electrode, GCE), a platinum wire as a counter electrode and an $Ag/AgCl/KCl_{sat}$ as a reference electrode. The prepared electrodes were characterized by scanning electron microscopic (SEM) (XLC Philips, Amsterdam, The Netherlands), transmission electron microscopic (TEM) (CH 200 Philips, Amsterdam, The Netherlands), X–ray diffraction (XRD) (Advanced D8 Brucker, Germany), atomic force microscopic (AFM) (Brucker Nano Instrument, Germany) and FT–IR spectroscopy (Jasco, Japan). The solid sample spectrum was obtained using KBr pellets.

2.3. Preparation of MWCNTs–modified GCE

First, MWCNTs were purified and activated in the HNO_3 solution to remove any residual metal impurities and to increase the surface area of the carboxylic functional groups. 3.0 g of MWCNTs with 25 mL 3.0 mol L^{-1} HNO_3 was placed into a 50 mL flask and refluxed for 15 h. The MWCNTs were subsequently washed with distillated water and dried at room temperature. The stable suspension of MWCNTs was prepared by dispersing the MWCNTs in N,N-dimethylformamide (DMF) (0.10 mg MWCNTs per 5 mL) using the ultrasonic bath. On

the other hand, an unmodified GCE was polished with alumina powder (0.05 μm) slurry for 3 min using a polishing cloth. It was then placed in an ethanol/water solution in an ultrasonic bath for 3 min before it was rinsed with water. Finally, 25 μL of the MWCNTs suspension was dropped onto the surface of the GCE to prepare the MWCNTs–GCE which was then dried at 30 ºC.[49]

2.4. Synthesis of $NiFe_2O_4$–MWCNTs nanocomposite

The citrate gel method was used for the chemical synthesis of $NiFe_2O_4$–MWCNTs nanocomposite. First, a mixture of 10 mL of 0.5 mol L^{-1} $Ni(NO_3)_2{\cdot}H_2O$ and 10 mL of 1.0 mol L^{-1} $Fe(NO_3)_3{\cdot}9H_2O$ was mixed well. Then, 0.75 g of the activated MWCNTs with 10 mL of 1.0 mol L^{-1} citric acid was added to the above mixture and ultrasonicated at room temperature for 10 min. The mixture was then stirred at 30 ºC for 48 h in NH_4OH solution (0.1 mol L^{-1}, pH 9.0) and the reaction mixture was dried in an oven at 100 ºC for 24 h. The product was calcinated at 620 ºC at a temperature increment rate of 10 ºC min^{-1} and the mixture was stored at 620 ºC for 2 h in argon atmosphere to produce the $NiFe_2O_4$–MWCNTs nanocomposite. Finally, 1.0 mg of $NiFe_2O_4$–MWCNTs was dispersed in 1.0 mL of methanol accompanied by ultrasonic agitation to obtain a well-dispersed suspension.[49]

2.5. Preparation of $NiFe_2O_4$–MWCNTs modified–GCE

Prior to each experiment, a GCE was polished to a mirror-like surface with alumina powder (Al_2O_3, 0.05 μm) in water using a polishing cloth. Then, the GCE was ultrasonicated in a solution of water-ethanol (50% v/v) for 3 min after each polishing step and washed with water. To prepare the $NiFe_2O_4$–MWCNTs modified–GCE, a micropipette (10 – 100 μL) was

used to drop 25 μL of the $NiFe_2O_4$–MWCNTs suspension onto the surface of the GCE and the resulting product was dried in airflow at 30 ºC.

2.6. Preparation of real samples

An injection solution (0.2 mg mL^{-1}) was prepared and 0.1 mL of the solution plus 10 mL of 0.1 mol L^{-1} buffer (pH 6.0) solution were used for analysis.

Blood and urine samples were stored in a refrigerator (at 4 °C) immediately after collection. Ten milliliter of each sample was centrifuged for 10 min at 3000 rpm. The supernatant was filtered using a 0.45 μm filter and diluted 1-time with the phosphate solution (pH 6.0). The solution was transferred into the voltammetric cell to be analyzed without any further pretreatment. The standard addition method was used for the determination of epinephrine content.

A HPLC method[50] was used to check the accuracy of the proposed method for real sample analysis. Reversed-phase HPLC with fluorescence detector and C18-column after pre-column derivatization using *o*-phthalaldehyde and 2-mercaptoethanol. Methanol and deionized water (in 0.1% acetic acid, v/v) with a ratio of 60:40 with flow rate was 0.8 mL min^{-1} was used as a mobile phase.

3. Results and discussion

3.1. Morphology and structure of $NiFe_2O_4$–MWCNTs

Fig. 1A displays a typical morphology of the modified nanocomposite GCE characterized by SEM. Fig. 1B clearly shows the deposition of $NiFe_2O_4$ magnetic nanoparticles in MWCNTs

as characterized by TEM. Clearly, the MWCNTs formed a tubular-like structure and $NiFe_2O_4$–MWCNTs developed into a porous structure. **"Here Fig. 1"**

Fig. 2 shows an AFM topology of $NiFe_2O_4$–MWCNTs corresponding to 2D (Fig. 2a) and 3D (Fig. 2b) images registered over an area of 1×1 μm. In the 3D AFM image, particles about 30 nm in size are clearly seen on the surface of $NiFe_2O_4$–MWCNTs nanocomposite.

"Here Fig. 2"

The XRD spectrum of $NiFe_2O_4$–MWCNTs magnetic nanocomposite displays eleven characteristic peaks at 2θ.[51] The diffraction peaks at 2θ of 26.27°, 43.42°, and 53.92° are the typical Bragg peaks of primitive CNTs and can be indexed to (002), (101) and (004), to reflect the presence of MWCNTs. This indicates that the magnetic nanoparticles are pure $NiFe_2O_4$–MWCNTs with a spinal structure. The JCPDS card number of the spinel NiFe2O4 is added as a supplementary material. The nanoparticles are in the range of 30 to 40 nm in size as calculated by Scherer Equation (Fig. 3). "**Here Fig. 3"**

The magnetic specification of the nanocomposite was evaluated in the fields of ±10 kOe at room temperature. The values for the retentivity (M_R), coercivity (H_C), and saturation magnetization (M_S) characterized by the VSM data were equal to 8.88 emu g^{-1}, 195.0 Oe, and 30.27 emu g^{-1}, respectively.

FT–IR spectrum (in the range of 4000–400 cm^{-1}) of the MWCNTs decorated with $NiFe_2O_4$ (Fig. 4) clearly displays adsorption bonds around 3436 cm^{-1}, which is attributed to the stretching vibration in the hydroxyl functional groups (O–H) on the surface of MWCNTs or the water adsorbed in the sample. The absorption bond at 1736 cm^{-1} corresponds to the stretching vibration of the carbonyl group (C=O). The stretching vibration of the carboxylate and ester groups (C=O) can be seen around 1622 cm^{-1} and that of the (C=C) group is located

at 1383 cm^{-1} while the absorption bond around 2920 cm^{-1} is attributed to the C–H stretching vibration. The absorption bond around 1100 cm^{-1} is assigned to the stretching vibration of the (C–C–C) group. Moreover, the two absorption bonds around 582 cm^{-1} and 439 cm^{-1} correspond to the vibration of tetrahedral and octahedral complexes' receptivity, which indicate the formation of spinal ferrite structure.[51–53] As can be observed in the FT–IR spectra, the normal mode of vibration of the tetrahedral cluster (582 cm^{-1}) is higher than that of the octahedral one (439 cm^{-1}); this can be due to the shorter bond length of the tetrahedral cluster than that of the octahedral one.

"Here Fig. 4"

3.2. Electrochemical behavior of epinephrine at electrode surfaces

The electrochemical properties of epinephrine were characterized at an unmodified-GCE and a $NiFe_2O_4$–MWCNTs–GCE by DPV in a phosphate solution (pH 4.0). The initial and final potentials were adjusted at 0.00 to +0.60 V, respectively, *vs.* Ag/AgCl. Fig. 5 shows the DPVs of 80.0 μmol L^{-1} epinephrine at the surface of $NiFe_2O_4$–MWCNTs–GCE (curve f), at MWCNTs–GCE (curve e), and at an unmodified-GCE (curve d). These voltammograms confirm that epinephrine exhibited a poor electrochemical response at the unmodified-GCE, whereas the epinephrine peak current increased sharply at the surface of the $NiFe_2O_4$–MWCNTs–GCE. The DP voltammograms of the blank solution (in the absence of epinephrine) at the unmodified-GCE, the MWCNTs–GCE, and the $NiFe_2O_4$–MWCNTs–GCE are shown in curves (a), (b), and (c), respectively, in Fig. 5. These results confirm that the increase in peak current is attributed to the synergic effect of $NiFe_2O_4$–MWCNTs nanocomposite on the oxidation of epinephrine.

The microscopic areas of the $NiFe_2O_4$–MWCNTs–GCE, the MWCNTs–GCE, and the unmodified-GCE were calculated based on the slope of the I_p *vs.* $\nu^{1/2}$ plot for a known concentration of $K_3Fe(CN)_6$ using the Randles–Sevcik Equation at a temperature of 25 ^oC:

$$I_p = (2.69\times10^5)An^{3/2}D_R^{1/2}C_s\nu^{1/2} \quad (1)$$

where, I_p refers to the peak current, A refers to the effective surface area of the electrode, n refers to the electron transfer number, D_R refers to the diffusion coefficient, C_s refers to the concentration of $K_3Fe(CN)_6$, and ν is the scan rate. In this case, 1.0 mmol L^{-1} $K_3Fe(CN)_6$ was used in the presence of 0.1 mol L^{-1} KCl electrolyte with n = 1 and $D_R = 7.6 \times 10^{-6}$ cm^2 s^{-1}. Based on the results obtained, the active surface areas of the unmodified-GCE, the MWCNTs–GCE, and the $NiFe_2O_4$–MWCNTs–GCE were equal to 0.0391, 0.1523, and 0.2326 cm^2, respectively. Using the same results, it is clear that the surface area of the MWCNTs–GCE and $NiFe_2O_4$–MWCNTs–GCE, respectively, are about 3.9 and 6.0 times greater than that of the unmodified-GCE. Using the nanocomposite on the surface of GCE increases the active surface area of the electrode, which in turn enhances the synergic effect of the nanocomposite on the oxidation of epinephrine. **"Here Fig. 5"**

3.3. Optimization of the variables on the sensor response

The relationship between the peak potential of epinephrine and the buffer solution pH at the $NiFe_2O_4$–MWCNTs–GCE was explored. To investigate the influence of pH on the oxidation peak potential and the peak current, samples of epinephrine each 20.0 μmol L^{-1} in volume and with different pH levels ranging from 3.0 to 9.0 (using phosphate solutions, 0.1 mol L^{-1}) were selected. The results (Fig. 6A) showed that the anodic peak current of epinephrine increased with increasing solution pH reaching its maximum value at pH 6.0 before it declined.

Therefore, pH 6.0 was chosen as the optimum pH level for the determination of epinephrine. Fig. 6B shows the oxidation peak potential of epinephrine at the surface of the $NiFe_2O_4$–MWCNTs–GCE for different pH levels. Clearly, the peak potential of epinephrine at the surface of the $NiFe_2O_4$–MWCNTs–GCE shifted to less positive values with increasing solution pH. Variation of the peak potential with pH was linear with a slope of 64 mV pH^{-1} and a correlation coefficient of 0.9932, which is close to that given by the Nernstian equation for equal number of electrons and protons transfer processes.[54] This behavior confirms that the numbers of electrons and protons in the oxidation reaction of epinephrine are the same[54,57,58] and are equal to two (Scheme 1). **"Here Fig. 6 and Scheme 1"**

The DP voltammograms of 50 μmol L^{-1} epinephrine at different scanning rates (pH 6.0) were investigated at the surface of $NiFe_2O_4$–MWCNTs–GCE. The results showed that the peak current of epinephrine increased gradually when scan rate increased from 10 to 70 mV s^{-1} (results not shown). This indicates a good linear relationship between peak currents and scan rates with a regression equation of $I_p(\mu A) = 2.47 + 13.7\nu(mV\ s^{-1})$, r = 0.9928. Further, it confirms that the oxidation of epinephrine at the surface of the modified electrode is controlled by the adsorption process.

The effect of accumulation potential on the oxidation peak current of epinephrine at the $NiFe_2O_4$–MWCNTs–GCE was studied in the range of 0.00 to 0.30 V using 10.0 μmol L^{-1} epinephrine at pH 6.0 over an accumulation time of 30s. The results indicate that the oxidation peak current increased with increasing accumulation potential from 0.00 to +0.05, whereas any greater accumulation potential led to a decreasing oxidation peak current. An optimal accumulation potential of 0.05 V was, therefore, selected for further experiments. Moreover, the influence of accumulation time on the oxidation peak current of epinephrine

was evaluated for an accumulation potential of +0.05 V and in the presence of 10.0 μmol L^{-1} epinephrine (pH 6.0). The results show that oxidation peak currents increased as a result of increasing accumulation time from 0 to 70 s before they leveled off. Therefore, 70 s was selected as the suitable accumulation time.

DPV parameters such as pulse amplitude and pulse time were optimized using the peak current of the oxidation of 10.0 μmol L^{-1} epinephrine in 0.1 mol L^{-1} phosphate solution (pH 6.0) at the $NiFe_2O_4$–MWCNTs–GCE. The optimization process led to the selection of a pulse amplitude of 80 mV and a pulse time of 50 ms.

3.4. Calibration plot, reproducibility, and stability

Fig. 7 shows the DP voltammograms of the modified electrode for different concentrations of epinephrine. The results indicate that the peak currents of epinephrine are proportional to its concentration in the two linear segments but with different slopes. The linear regression equation for the range of 0.9–40.0 μmol L^{-1} of epinephrine was $I_p(\mu A) = 0.0395C_{ep} + 0.060$ ($r^2 = 0.9961$), and it was $I_p(\mu A) = 0.0194C_{ep} + 0.4770$ ($r^2 = 0.9972$) for the range 40.0–800.0 μmol L^{-1} of epinephrine. The number of repeats in the calibration plots was 3. In these equations, C_{ep} is μmol L^{-1} concentration of epinephrine and I_p is the peak current. The detection limit defined as (S/m) (where S is the standard deviation of the y–intercept and m is the slope of the regression lines) was found to be 0.09 μmol L^{-1} epinephrine. **"Here Fig. 7"**

The reproducibility and stability of the $NiFe_2O_4$–MWCNTs–GCE were determined for six successive assays of 10.0 μmol L^{-1} epinephrine at the $NiFe_2O_4$–MWCNTs–GCE sensor. The relative standard deviation (RSD%) was calculated based on the experimental results equal to 1.3%. When using five different electrodes, the RSD% for five measurements was

1.5%. When the electrode was stored in the laboratory, the modified electrode retained 98% of its initial response after a week and 96% after 45 days. These results indicate that the $NiFe_2O_4$–MWCNTs–GCE sensor is both stable and reproducible. Table 1 shows both the advantages and the disadvantages of the proposed electrochemical sensor over the electrochemical methods reported for the detection of epinephrine. As can be seen from the Table, the proposed method has a comparable or better performance with respect to the parameters involved in epinephrine determination. **"Here Table 1"**

3.5. Interference study

In order to evaluate the selectivity of the proposed electrochemical sensor for the determination of epinephrine, the influence of various foreign species on the determination of 10.0 μmol L^{-1} epinephrine were evaluated under optimum conditions. The tolerance limit was taken as the maximum concentration of the foreign materials causing approximately ±5% relative error in the determination of epinephrine. The results provided in Table 2 show that different cations, anions, amino acids, and organic substances failed to affect the selectivity of the sensor. However, dopamine was found to interfere at more than 50-fold. Fig. 8 shows the sensor responses to 10.0 μmol L^{-1} epinephrine in the presence of 300 μmol L^{-1} ascorbic acid, 100 μmol L^{-1} uric acid, and 50 μmol L^{-1} dopamine. **“Here Fig. 8 & Table. 2”**

4. Real sample analysis

In order to evaluate the applicability of the proposed electrochemical sensor for the determination of epinephrine by DPV in real samples, the ability of the electrochemical sensor for the determination of epinephrine was examined in samples of injection solution,

blood plasma, and urine using the standard addition method. The results of the analyses are summarized in Table 3. The accuracy of the proposed electrochemical sensor in real samples was also investigated using the HPLC method[50]. The results obtained indicate that the proposed electrochemical sensor has a good precision, accuracy, and recovery.

"Here Table 3"

5. Conclusion

In this article, a new electrochemical sensor based on $NiFe_2O_4$–MWCNTs nanocomposite was introduced for the sensitive determination of epinephrine. An adsorption process was found to occur during the redox process of epinephrine at the surface of the modified electrode. The electrochemical responses of epinephrine showed that the nanocomposite has a higher surface area and exhibits a strong synergic effect on the oxidation of epinephrine. Moreover, the sensor was found to have a satisfactory sensitivity and a long linear dynamic range with an experimental detection limit of as low as 0.09 μmol L^{-1}. According to the reported electrochemical methods for epinephrine detection, the proposed sensor has a good sensitivity, lower detection limit, good stability and free from interference of ascorbic acid and uric acid. The proposed method can, therefore, be recommended for use as a novel electrochemical sensor for epinephrine analysis in pharmaceutical and body fluids with a satisfactory accuracy.

Acknowledgment

The authors wish to thanks Isfahan University of Technology (IUT) Research Council, the Iranian Nanotechnology Council, the Center of Excellence in Sensor and Green Chemistry for supporting of this work.

References

1. Y. Kinemuchi, K. Ishizaka, H. Suematsu, W. H. Jiang, K. Yatsui, *Thin Solid Films* **2002**, 407, 109.

2. Y. L. Liu, H. Wang, Y. Yang, Z. M. Liu, H. F. Yang, G. L. Shen, R. Q. Yu, *Sens. Actuators B* **2004**, 102, 148.

3. L. Yang, Y. Xie, H. Zhao, X. Wu, Y. Wang, *Solid-State Electronics* **2005**, 49, 1029.

4. L. Luo, Q. Li, Y. Xu, Y. D. X. Wang, D. Deng, Y. Xu, *Sens. Actuators B* **2010**, 145, 293.

5. P. Kim, S. Agnihotri, *J. Colloid Interf. Sci.* **2008**, 325, 64.

6. P. Ajayan, O. Zhou, Top. *Appl. Phys.* **2001**, 80, 391.

7. E. Bakalis, F. Zerbetto, *Chem. Phys. Lett.* **2008**, 463, 139.

8. B. Salimi, B. Kavosi, R. Hallaj, A. Babaei, *Electroanalysis* **2009**, 21, 909.

9. T. Hemraj-Benny, T. J. Bandosz, S. S. Wong, *J. Colloid Interf. Sci.* **2008**, 317, 375.

10. M. Sagnes, J. M. Broto, B. Raquet, C. Vieu, V. Conedera, P. Dubreuil, T. Ondarcuhu, Ch. Laurent, E. Flahaut, *Microelectron Eng.* **2004**, 73, 689.

11. A. A. Ensafi, H. Karimi-Maleh, S. Mallakpour, B. Rezaei, *Colloids Surf. B* **2011**, 87, 480.

12. A. A. Ensafi, M. Taei, H.R. Rahmani, T. Khayamian, *Electrochim. Acta* **2011**, 56, 8176.

13. A. A. Ensafi, H. Karimi-Maleh, *Electroanalysis* **2010**, 22, 2558.

14. C. Li, E. T. Thostenson, T. W. Chou, *Compos. Sci. Technol.* **2008**, 68, 1227.

15. J. J. Xu, X. L. Luo, Y. Du, H. Y. Chen, *Electrochem. Commun.* **2004**, 6, 1169.

16. C. Y. Wang, X. Y. Hu, *Talanta* **2005**, 67, 625.

17. C. Huiqun, Z. Meifang, L. Yaogang, *J. Magn.* Magn. *Mater.* **2006**, 305, 321.

18. Y. Zhan, R. Zhao, Y. Lei, F. Meng, J. Zhong, X. Liu, *J. Magn.* Magn. *Mater.* **2011**, 323, 1006.

19. B. P. Jia, L. Gao, J. Sun, *Carbon* **2007**, 45, 1476.

20. Y. Liu, W. Jiang, Y. Wang, X. J. Zhang, D. Song, F. S. Li, , *J. Magn.* Magn. *Mater.* **2009**, 321, 408.

21. Q. M. Xue, *Physiological and Pathological Chemistry of Nervous System*, Science Press, Beijing, **1978**.

22. W. A. Banks, *Brain Res.* **2001**, 899, 209.

23. L. Jackson, F. L. R. Williams, A. Burchell, M. W. H. Coughtrie, R. Hume, *J. Clin. Endocr. Metab.* **2004**, 89, 6251.

24. A. A. Ensafi, M. Taei, T. Khayamian, *Colloids Surf. B* **2010**, 79, 480.

25. M. A. Fotopoulou, P. C. Loannou, *Anal. Chim. Acta* **2002**, 462, 179.

26. S. Shelkovnikov, H. C. Gonick, *Life Sci.* **2004**, 75, 2765.

27. V. Carrera, E. Sabater, E. Vilanova, M. A. Sogorb, *J. Chromatogr. B* **2007**, 847, 88.

28. X. Zhu, P.N. Shaw, D. A. Barrett, *Anal. Chim. Acta* **2003**, 478, 259.

29. F. Ferreira, L. Silva, A. C. Freitas, A. C. Duarte, *J. Chromatogr. A* **2009**, 1216, 7049.

30. L. I. B. Silva, F. D. P. Ferreira, A. C. Freitas, T. A. P. R. Santos, A. C. Duarte, *Talanta* **2009**, 80, 853.

31. L. Y. Zhang, S. F. Qv, Z. L. Wang, J. K. Cheng, *J. Chromatogr. B* **2003**, 792, 381.

32. S. L. Wei, G. Q. Song, J. M. Li, *J. Chromatogr. A* **2005**, 1098, 166.

33. E. M. Garrido, J. L. Lima, D. M. Cristina, *J. Pharm. Biomed. Anal.* **1997**, 15, 845.

34. J. J. Willemsen, H. A. Ross, M. C. Jacobs, W. M. Lenders, Th. Thien, *Clin. Chem.* **1995**, 41, 1455.

35. Y. Y. Su, J. Wang, G.N. Chen, *Talanta* **2005**, 65, 531.

36. J. Michalowski, P. Halaburda, *Talanta* **2001**, 55, 1165.

37. M. H. Sorouraddin, J. L. Manzoori, E. Kargarzadeh, et al., *J. Pharm. Biomed. Anal.* **1998**, 18, 877.

38. M. Zhu, X. M. Huang, J. Li, et al., *Anal. Chim. Acta* **1997**, 357, 261.

39. Y. Wang, Z. Z. Chen, *Colloids Surf. B* **2009**, 74, 322.

40. D. Brondani, C. Scheeren, J. Dupont, I. C. Vieira, *Sens. Actuators B* **2009**, 140, 252.

41. C. W. Hsu, M. C. Yang, *Sens. Actuators B* **2008**, 134, 680.

42. S. H. Kim, J. W. Lee, I. H. Yeo, *Electrochim. Acta* **2000**, 45, 2889.

43. H. Karimi maleh, M. A. Khalilzadeh, T. Tavana, A. A. Ensafi, H. Beitollahi, D. Zareyee, *J. Mol. Liq.* **2012**, 168, 69.

44. X. Liu, D. Ye, L. Luo, Y. Ding, Y. Wang, Y. Chu, *J. Electroanal. Chem.* **2012**, 665, 1.

45. P. Hernandez, I. Sanchez, F. Paton, L. Hernandez, *Talanta* **1998**, 46, 985.

46. F. Cui, X. Zhang, *J. Electroanal. Chem.* **2012**, 669, 35.

47. A. A. Ensafi, A. R. Allafchian, *Colloids Surf. B* **2013**, 102, 687.

48. A. A. Ensafi, B. Arashpour, B. Rezaei, A. R. Allafchian *Mater. Sci. Eng. C* **2014**, 39, 78.

49. A. A. Ensafi, A. R. Allafchian, B. Rezaei, R. Mohammadzadeh, *Mater. Sci. Eng. C* **2013**, 33, 202.

50. H. X. Zhao, H. Mu, Y. H. Bai, H. Yu, Y. M. Hu, *J. Pharma. Anal.* **2011**, 1, 208.

51. R. D. Waldron, *Phys. Rev.* **1955**, 99, 1727.

52. S. Maensiri, C. H. Masingboon, B. Boonchom, S. Seraphin, *Scripta Mater.* **2007**, 56, 797.

53. A. A. Ensafi, M. Jafari-Asl, B. Rezaei, A. R. Allafchian, *Sens. Actuatours B* **2013**, 177, 634.

54. P. Vijaybhaskar, A. Ramachandrailah, *Eur. J. Chem.* **2009**, 6, 1181.

55. Y. B. He, H. Q. Luo, N. B. Li, *Instrum. Sci. Technol.* **2007**, 35, 163.

56. R. Wang, Q. L. Hong, B. L. Nian, *Biosens. Bioelectron.* **2006**, 21, 1086.

57. F. C. Moraes, D. L. C. Golinelli, L. H. Mascaro, and S. A. S. Machado, *Sens. Actuators B* **2010**, 148, 492.

58. M. E. Ghica, Ch. M. A. Brett, *Anal. Lett.* **2013**, 46, 1379.

Table 1 Comparison of the proposed electrochemical sensor with the reported voltammetry methods for the determination of epinephrine.

Technique	Type of electrode	Limit of detection ($\mu mol\ L^{-1}$)	Linear range ($\mu mol\ L^{-1}$)	RSD%	Interfering compounds	Reference
Cyclic voltammetry	Modified-GCE	0.3	2.0 – 600.0	2.13	Lysine, cystine, glycin, citric acid	39
DPV	MnO_2/Nafion/GCE	0.05	0.3-100	0.86	dopamine	44
Cyclic voltammetry	GR/Au/GCE	0.07	0.5–8.0	---	Not study	46
Cyclic voltammetry	Au	0.39	0.5 – 800.0	1.6	Zn^{2+}, Al^{3+}	55
Cyclic voltammetry	Modified-GCE	0.2	2.0 – 80.0	2	Not study	56
DPV	Paraffin/MWCNT/CoPc	0.016	1.3–5.5	---	Not study	57
DPV	MWCNT/CFE	0.900	up to 100	8.3	Not study	58
DPV	$NiFe_2O_4$–MWCNTs–GCE	0.09	0.1 – 1000.0	0.9	–	This work

Table 2 Interference study under the optimum conditions.

Species	Tolerance limit ($W_{substance}/W_{analyte}$)
Glucose, Sucrose, Fructose, Lactose, Na^+, K^+, Ca^{2+}, Mg^{2+}, Cl^-, F^-, Br^-, NO_3^-	1000*
Salicylic acid, citric acid	600
Valine, Histidine, Glycin, Leusine	400
Ascorbic acid, Urea	300
Methionine, Uric acid	100
Dopamine	50
Starch	Saturation

*maximum concentration of tested spices.

Table 3 Determination of epinephrine in real sample at pH 6.0 (n = 3).

Sample	Epinephrine added ($\mu mol\ L^{-1}$)	Epinephrine found ($\mu mol\ L^{-1}$)	Recovery (%)	HPLC ($\mu mol\ L^{-1}$)
Injection solution	65.0	64.0 ± 0.2	98.5	63.1 ± 0.1
Plasma	50.0	48.7 ± 0.1	97.4	50.8 ± 0.1
Plasma	9.0	8.8 ± 0.2	97.6	8.9 ± 0.8
Urine	50.0	51.5 ± 0.5	103.0	51.1 ± 0.2
Urine	9.0	8.9 ± 0.1	98.4	9.1 ± 0.1

± shows the standard deviation (n = 3).

Legends for the figures

Fig. 1. A): SEM image of $NiFe_2O_4$–MWCNTs nanocomposite; B): TEM image of the MWCNTs decorated with $NiFe_2O_4$.

Fig. 2. a): 2D and b): 3D AFM topology of the surface of $NiFe_2O_4$–MWCNTs nanocomposite.

Fig. 3. X-ray diffraction patterns of the magnetic nanocomposite.

Fig. 4. FT-IR spectra of $NiFe_2O_4$–MWCNTs nanocomposite.

Fig. 5. Voltammetric response of the electrolyte: a) at the bare GCE; b) at MWCNTs modified GCE; and c) at $NiFe_2O_4$–MWCNTs modified GCE. Voltammetric response of 80.0 μmol L^{-1} epinephrine at d): a bare GCE; e) the MWCNTs modified GCE; and f) at the $NiFe_2O_4$–MWCNT modified GCE. Conditions: phosphate solution, 0.1 mol L^{-1}, pH 4.0; and scan rate of 50 mV s^{-1}.

Fig. 6. A) Relationship between the solution pH and the peak current; B) Influence of the solution pH on the peak potential of epinephrine (20.0 μmol L^{-1}).

Fig. 7. Calibration curves for epinephrine at pH 6.0 under the optimum conditions for 0.9 to 800.0 μmol L^{-1} (n = 3). Inset: Voltammograms of various concentrations of epinephrine as (1–14 corresponding to 0.9 – 800.0 μmol L^{-1} epinephrine).

Fig. 8. DPVs of a): 10.0 μmol L^{-1} epinephrine; b): 10.0 μmol L^{-1} epinephrine in the presence of 300.0 μmol L^{-1} ascorbic acid; c): 10.0 μmol L^{-1} epinephrine in the presence of 100.0 μmol L^{-1} uric acid; and d): 10.0 μmol L^{-1} epinephrine in the presence of 50.0 μmol L^{-1} dopamine.

Scheme 1. A proposed mechanism for the oxidation of epinephrine at the surface of the modified electrode.